JOURNAL OF Applied Polymer SCIENCE

Synthesis and Characterization of PLA Nanocomposites Containing Nanosilica Modified with Different Organosilanes I. Effect of the Organosilanes on the Properties of Nanocomposites: Macromolecular, Morphological, and Rheologic Characterization

Luca Basilissi, Giuseppe Di Silvestro, Hermes Farina, Marco Aldo Ortenzi
Università degli Studi di Milano, Dipartimento di Chimica, Via Venezian 21, I-20133, Milano, Italy
Correspondence to: L. Basilissi (E-mail: luca.basilissi@unimi.it)

ABSTRACT: Polylactide nanocomposites containing different loadings of nanosilica were prepared by employing bulk ring opening polymerization from lactide. Nanosilica was used as such and after surface treatment with different amounts of two distinct silanes. The effects on the properties of the material were evaluated comparing the samples containing organosilane-modified nanosilica with poly(-lactic acid) (PLA) containing unmodified nanosilica. A standard linear PLA and an industrial "film grade" PLA (PLA Natureworks 4032D) were used as reference. Pure silica tends to decrease the molecular weight of the material, deactivating the catalytic system but when silanes are present on the surface, molecular weights are similar to the ones of standard and industrial PLA. Transmission electron microscopy analysis shows that silanes improve the dispersion of the mineral, while rheologic curves suggest that when silanes are present melt viscosity increases markedly at zero shear and decreases faster as the shear rate increases. © 2012 Wiley Periodicals, Inc. J. Appl. Polym. Sci. 000: 000–000, 2012

KEYWORDS: nanostructured polymers; biopolymers and renewable polymers; packaging

Received 5 April 2012; accepted 4 July 2012; published online
DOI: 10.1002/app.38324

INTRODUCTION

The need to solve the problems caused by oil deriving plastic materials, including waste treatment, has forced both industrial and academic research to develop new environmentally friendly polymers; aliphatic polyesters are among the most promising polymers of this kind and some of them (i.e., polycaprolacton or polyglycolic acid) have been used for the last 20 years in many biomedical applications thanks to their biocompatibility and biodegradability.

Poly(lactic acid) (PLA) is a biodegradable, biocompatible, and compostable semicrystalline polyester deriving from lactic acid. As the monomer (L-lactide) can be obtained from renewable sources, PLA has received much attention from the industrial world as an alternative to traditional polymers not only in the biomedical field but also for engineering plastic applications; even if PLA has some features very similar to the ones of polyolefins,[1,2] it is quite brittle and presents an high permeability toward gases;[3,4] thus limiting its use for many industrial applications (i.e., packaging).

The addition of small quantities (0.5–5% w/w) of nanoparticles such as silica,[5] carbon nanotubes,[6] graphite,[7] montmorillonite[8] to the polymeric matrix has been widely studied to improve some properties of many polymeric materials. The low dimensions of nanoparticles and their relatively high surface area can give to a nanocomposite material improved features such as gas barrier properties,[9] mechanical strength, and thermal stability in comparison to the pure polymer; however, in order to have a nanocomposite material, the nanoparticle must be efficiently dispersed in the polymeric matrix without the presence of aggregates having micrometric dimensions.

Nanocomposite materials can be obtained via compounding[10] or via "in situ" polymerization; usually the latter guarantees an improved interaction and a better dispersion in the polymeric matrix.[11–13]

In the last years, the study of potentially biodegradable nanocomposites, mainly based on PLA polymers, has intensified, in order to improve the properties of the material and to find new applications.[14–17]

Among them, nanosilica/PLA nanocomposite materials seem to be very promising; most of the scientific literature deals with nanocomposites prepared via blending, using twin screw extruders to achieve an efficient dispersion of the mineral in the

Additional Supporting Information may be found in the online version of this article.

polymer[18,19], or dissolving and reprecipitating the polymeric matrix in a solvent containing nanosilica.[20,21] There are just a few papers related to the "in situ" preparation of PLA/nanosilica nanocomposites them.[22–24]

In this article (part I) and in a second one (part II), molecular, thermal, and rheological properties of PLA/silica nanocomposites obtained via "in situ" ring opening polymerization (ROP) of L-Lactide were evaluated; the nanocomposites have been obtained using both standard nanosilica and nanosilica modified with organosilanes. In order to improve the compatibility between the polymeric matrix and the inorganic surface of silica, organosilanes having amino and epoxy functional groups were chosen. In the first article, the effect of nanosilica on the molecular weight and on the rheological properties will be discussed. In the second article, thermal properties of these materials will be presented: crystallinity, crystallization kinetics, and thermal stability of PLA/nanosilica composites will be studied by differential scanning calorimetry (DSC) and thermogravimetric (TGA) analyses.

EXPERIMENTAL

Materials and Methods

PLA was synthesized from L-lactide, LL Purasorb Lactide (purity > 99.5%) purchased from Purac Biomaterials. Methylene chloride, methanol (HPLC purity), tin octanoate, and nanosilica with an average diameter of 10 nm and surface area of 590–690 m^2/g were purchased from Sigma-Aldrich Co. LLC. 3-Aminopropyltriethoxysilane (Geniosil GF93) and 3-glicidoxypropyltrimethoxysilane (Geniosil GF80) were purchased from Wacker Chemie AG. All the reagents were used without further purification. PLA 4032D is a commercial product of Natureworks, having an high optical purity, with about 98% L-lactide content. M_w declared is 250,000 Dalton with polydispersity of 1.70 according to size exclusion chromatography (SEC), polystyrene standards (PS).

The dispersion of nanosilica in the polymeric matrix was evaluated via transmission electron microscopy (TEM): samples were reduced into ultrathin sections of 80 nm by an Ultracut E microtome (Reichert), collected onto a 300 mesh copper grid and examined by an EFTEM Leo912ab TEM (Zeiss) operating at 80 kV. Digital images were acquired by Esivision CCD-BM/1K system. Crystalline lattices were observed via wide angle X-ray scattering (WAXS), using a Rigaku DMAX-II. Diffraction patterns were obtained in the range $5°<2\theta<50°$ with Cu-Kα radiation ($\lambda = 1.5405$ Å) under the following conditions; 40 kV, 40mA, step width 0.02°, time per step 2 sec, divergence slit 0.25°, soller slit 0.04 rad, antiscatter slit 0.5°. X-ray patterns shown in Figure 2 are normalized on the main peak.

The effect of silica on the molecular weight of the nanocomposites was evaluated using a SEC system having Waters 1515 Isocratic HPLC pump and a six styragel columns set (HR2-HR3-HR3-HR4-HR4-HR5) with a Waters 2487 Dual λ Absorbance Detector using a flow rate of 1 mL/min and 20 μL as injection volume; samples were prepared dissolving 30 mg of polymer in 1 mL of anhydrous CH_2Cl_2; before the analysis, the solution was filtered with 0.45 μm filters. Given the relatively high loading, a check was performed using lower concentrations of polymer (5 mg/mL), in order to verify that no column overloading could be observed. Anyway, higher loadings were preferred as UV signal of PLA is relatively weak.

Rheologic curves were collected using a Physica MCR 300 rotational rheometer; frequency sweep (from 100 Hz to 0.1 Hz) curves were obtained at 190°C, using a 25 mm plate–plate geometry with constant deformation of 5%; in the article, shear rate and not angular frequency is reported on the X-axis.

Table I. Quantity of Silanes Present on Silica Surface

Silane added (w/w % on silica)	meq/Kg measured
2.0% GF 93	148
7.5% GF 93	671
15.0% GF 93	1287
2.0% GF 80	146
7.5% GF 80	447
15.0% GF 80	798

Surface Modification of Nanosilica

In order to improve the compatibility between the polymeric matrix and the inorganic surface of silica, organosilanes having amino (GF93) and epoxy functional groups (GF80) were chosen.

For the surface modification, 20 g of nanosilica were dispersed in methanol (100 mL) under vigorous stirring. Silane was added dropwise (quantities w/w reported in Table I). The dispersion was left 12 h under stirring at room temperature, then methanol was evaporated under vacuum (9×10^{-2} torr); samples where then dried at 50°C overnight.

The quantity of organosilane effectively reacted on the surface of nanosilica (see Figure 1) was determined via potentiometric titration; silica modified with GF93 was characterized directly by neutralization of amino groups with HCl 0.01 N. The quantity of GF80 present on the silica surface was determined titrating the quantity of tertiary amine deriving from the reaction between the epoxy groups and *N*, *N* dibutylamine.

The GF80-modified silica was dispersed in a solution of *N*, *N*'-dibutylamine in methylene chloride; the dispersion was left at room temperature for 12 h and then the solvent was evaporated under vacuum. Free amine was eliminated under vacuum at 40°C for 1 h and silica was then dispersed in hot *m*-cresol and titrated with HCl 0.01 N in methanol.

In Table I the quantity of silanes determined via potentiometric titration of the terminal groups is reported.

The effect of surface modification of nanosilica was studied also using Fourier transformed infrared spectroscopy (FTIR).[25] The FTIR spectra of three nanosilica samples are reported in Supporting Information. Silane functional groups are not easy to detect due to the intense and broad peaks of Si—O (1020–1250 cm^{-1}) and —OH (3300–3700 cm^{-1}), but however, the intensity of the absorption peak between 3300 and 3700 cm^{-1} related to the presence of silanol group is lower in silane-modified silica

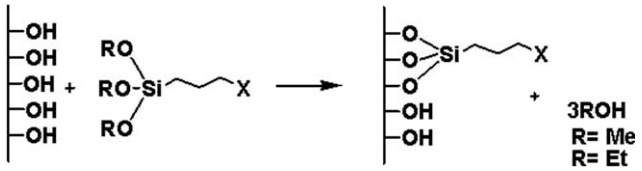

Figure 1. Reaction between silanes and silica surface.

in comparison unmodified silica, confirming that the functional groups of silanes are present on the surface.

Synthesis of PLA and PLA/Silica Nanocomposites

Pure PLA was synthesized in bulk using a 250 mL three-neck glass flask: 100 g of L-lactide were polymerized under nitrogen at 180°C for 2 h in the presence of tin octanoate (0,1% w/w) as catalyst, under mechanical stirring. L-lactide and tin octanoate were previously dried at 80°C under vacuum for 12 h. PLA/silica nanocomposites were synthesized using the same apparatus: L-lactide (100 g), nanosilica (0.5–1.0–2.0% w/w) and tin octanoate (0.1% w/w) were previously dried at 80°C under vacuum for 12 h.

Film Casting

Films for WAXS were obtained from a chloroform solution; 10 g of polymers were dissolved in 50 g of $CHCl_3$. The solution was cast on a glass surface and the solvent was evaporated at room temperature and pressure.

RESULTS AND DISCUSSION

Synthesized samples are listed in Table II: standard (STD) is a standard linear PLA, UMS samples contain unmodified nanosilica, GF93 and GF80 samples contain silica modified with amino or epoxy silane.

SEC Data

Molecular weights were determined via SEC; SEC system was calibrated with specifically in bulk synthesized linear PLAs. PLAs for SEC calibration were synthesized with the same procedure described in materials and methods section, using a monofunctional comonomer, tetradecanol, to control molecular weight values. M_n of these PLAs have been determined via ^{1}H NMR, as already reported in literature,[26] to be in the range between 1514 Daltons and 65,090 Daltons; the polynomial calibration curve was created using the M_n deriving from ^{1}H NMR analysis.

Table II. Samples Synthesized

Sample	Silica (% w/w on lactide)	Silane	Silane added (% w/w on silica)
STD			
0.5 UMS	0.5		
1.0 UMS	1.0		
2.0 UMS	2.0		
2.0 GF93	1.0	Amino (GF93)	2
7.5 GF93	1.0	Amino (GF93)	7.5
15.0 GF93	1.0	Amino (GF93)	15
2.0 GF80	1.0	Epoxy (GF80)	2
7.5 GF80	1.0	Epoxy (GF80)	7.5
15.0 GF80	1.0	Epoxy (GF80)	15

Table III. SEC Data of the Polymers Synthesized

Sample	M_n	M_w	D
4032D	58760	105771	1.80
STD	56720	104365	1.84
0.5 UMS	52422	106387	1.99
1.0 UMS	49357	86990	1.82
2.0 UMS	27503	41797	1.61
2.0 GF80	45800	84680	1.78
7.5 GF80	52014	105068	2.02
15.0 GF80	53194	105856	1.99
2.0 GF93	49380	98700	2.00
7.5 GF93	52000	101386	1.95
15.0 GF93	52115	91715	1.76
2.0 UMS 3.0 Sn	53813	97939	1.82

Our synthetic procedure was checked comparing Molecular weight of STD sample with the one of PLA Natureworks 4032D (4032D in Table III).

It is interesting to point out that our calibration gives M_n and M_w values for Natureworks 4032D far lower than the ones declared by the producer; polydispersity is not very different. The difference in molecular weights estimation is caused by the different hydrodynamic volume of polystyrene polymers (having a rigid aromatic group) in comparison to PLA. ^{1}H NMR on Natureworks 4032D indicates a M_n of about 55,010 therefore M_n obtained thanks to our calibration matches with this value far better than the one obtained using polystyrene (PS) calibration.

As described before, samples were filtered with a 0.45 μm filter, therefore molecular weight data refer only to the part of the polymer present in solution. Table III shows M_n and D values for PLA polymers synthesized. The three UMS samples evidence that the mineral interferes with the polymerization process, lowering the molecular weights as its quantity increases (M_n of 2.0 UMS is reduced to half in comparison to M_n of STD sample), as already reported in literature;[27] this phenomenon is due to the fact that —OH groups on the surface of unmodified nanosilica can initiate the polymerization. On the other hand, it should be noted that the —Si—O—C— bonds created between silica and the growing chain are easily hydrolized.[22] Conversions of polymerization reactions are very similar, as evidenced by NMR analyses (checking lactide peaks in comparison to those of the polymer) and by SEC analysis, that shows that lactide peaks areas are very similar for each sample; therefore, another explanation for the lowering of molecular weight of the samples with pure nanosilica might be that free acidic sites on the surface of nanosilica partially deactivate the catalyst. To confirm the validity of this assumption, a sample was synthesized containing a very high quantity of Sn octanoate (3% w/w) and 2% w/w of nanosilica (sample 2.0 UMS 3.0 Sn) whose M_n and M_w are close to the ones of STD sample.

Applied Polymer SCIENCE

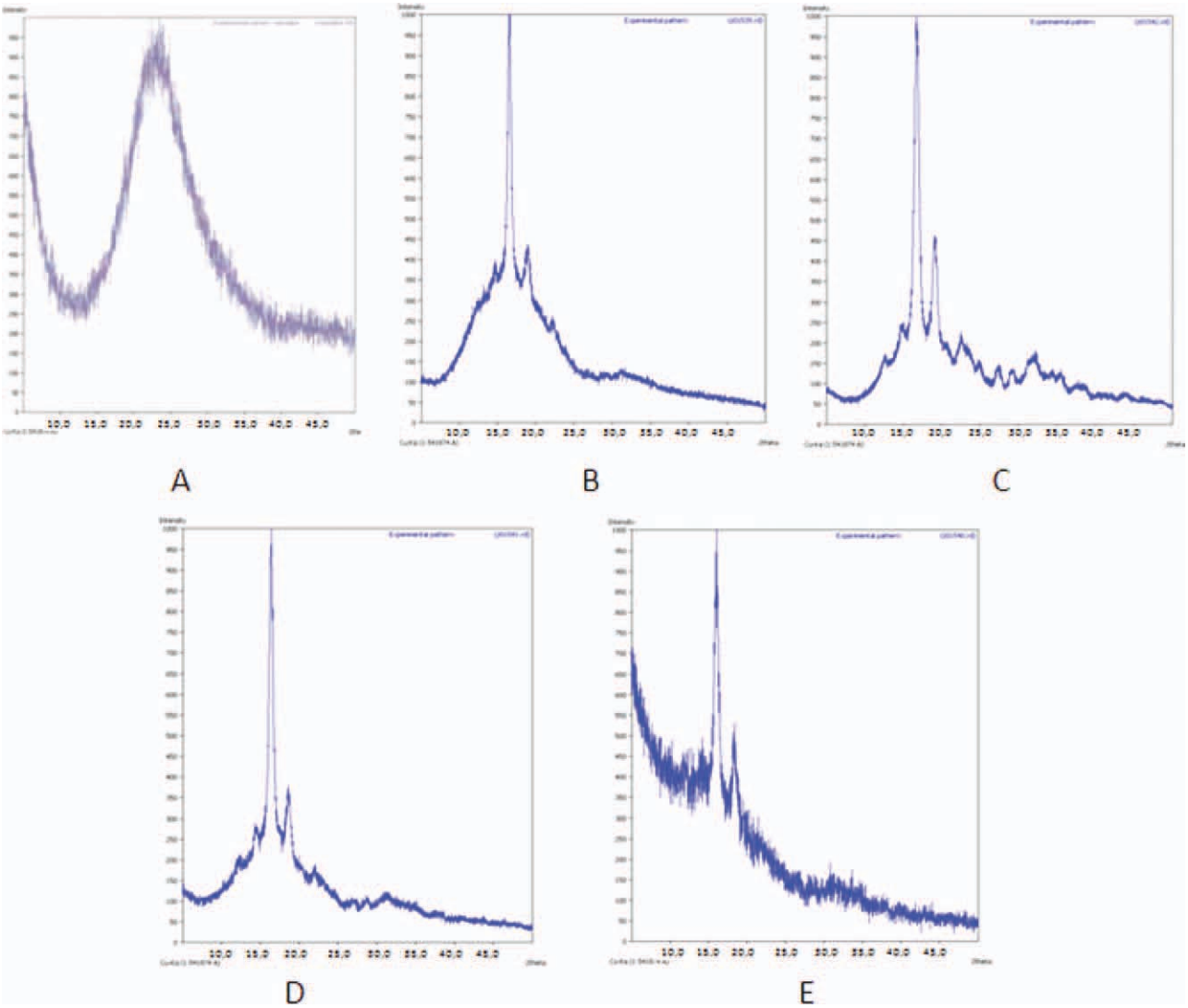

Figure 2. WAXS diffractograms of: Pure silica (a), STD film (b) 1.0 UMS film (c), 15.0 GF93 film (d), 15.0 GF80 film (e). [Color figure can be viewed in the online issue, which is available at wileyonlinelibrary.com].

On the other hand, nanocomposites containing surface modified silica have M_n comparable with the one of pure PLA, indicating that organosilanes eliminate the negative effect of nanosilica free —OH surface groups on the polymerization process reacting with them.

WAXS Analyses

The crystalline structure of PLA and of the nanocomposites was via WAXS analyses on films obtained by casting from PLA solutions in $CHCl_3$, as described. As shown in Figure 2, there are four characteristic peaks at $2\theta = 14.60°$, $16.68°$, $19.14°$, e $22.27°$, as already reported in literature.[28]

In the presence of unmodified nanosilica a shift of the peaks was not observed, but an increase of the intensity of peaks at $2\theta = 16.68°$ e $22.27°$ was recorded demonstrating an increase of crystallinity.

The observation of the WAXS of the nanocomposites obtained using the silica modified with silanes, seems to suggest that the interaction between the mineral and the polymeric matrix partially disturbs the crystallinity of the film; peaks have lower intensity in comparison to the UMS ones, especially when using GF80 as compatibilizer. Thermal behavior and crystallinity of the samples will be further discussed in more details in part II article.

TEM Images

Figure 3 shows TEM images of PLA/silica nanocomposites; unmodified silica [Figure 3(A)] is dispersed poorly in the matrix, forming micrometric aggregates that cause nonhomogeneity in the material. Figure 3(B,C) show that organosilanes give an improved compatibility with the organic matrix, resulting in a far better dispersion of silica particles in the material and therefore in an improved homogeneity.

Rheologic Curves

The rheologic curves obtained via frequency sweep experiments on PLA nanocomposites with unmodified silica are presented in

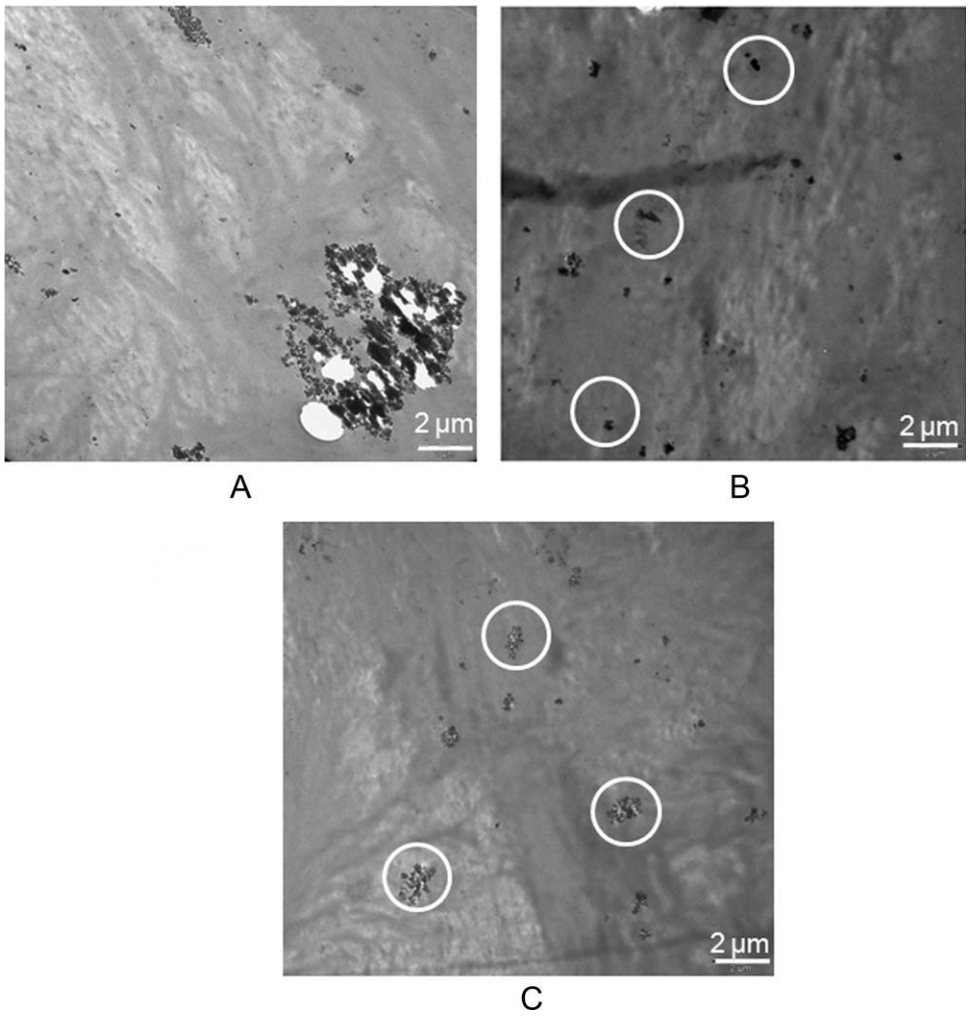

Figure 3. TEM images of 1.0 UMS (A), 7.5 GF93 (B) and 7.5 GF80 (C).

Figure 4. They present the standard newtonian plateau at low shear and a shear-thinning behavior at higher frequencies. η_0 values (shown in Table IV) have been calculated using cross equation [eq. (1)] passing from experimental data obtained as complex viscosity versus angular frequency to data as standard shear viscosity versus shear rate thanks to Cox-Merz rule. In eq. (1), η_0 represents zero shear viscosity, η_∞ is infinite-shear viscosity, $\dot{\gamma}$ is shear rate, (1-n) is known as cross rate constant, is dimensionless, and is a measure of the degree of dependence of viscosity on shear rate in the shear-thinning region and K is known as the cross time constant and has dimensions of time.

$$\frac{\eta-\eta_\infty}{\eta_0-\eta_\infty}=\frac{1}{1+\left(K^2\cdot\dot{\gamma}^2\right)^{\frac{1-n}{2}}}=\frac{1}{1+\left(K\cdot\dot{\gamma}\right)^{1-n}} \qquad (1)$$

Natureworks 4032D and our STD sample present similar complex viscosity and similar η_0 values. As expected, the presence of inorganic particles increases the viscosity of the melt;[29] although 0.5 and 1.0 UMS have molecular weight similar to linear standard PLA, they are characterized by a much higher η_0; noteworthy

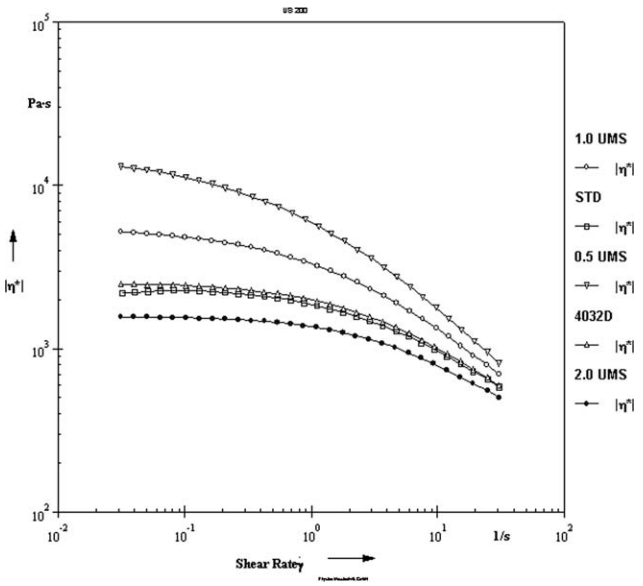

Figure 4. Rheology of standard PLA and of UMS samples.

Applied Polymer SCIENCE

Table IV. η_0 of the Samples Synthesized

Sample	η_0 (Pa×s)
Nature works 4032D	2.48×10^3
STD	2.19×10^3
0.5 UMS	1.30×10^4
1.0 UMS	5.19×10^3
2.0 UMS	1.56×10^3
2.0 GF80	7.52×10^3
7.5 GF80	1.10×10^4
15.0 GF80	1.47×10^4
2.0 GF93	5.98×10^3
7.5 GF93	1.34×10^4
15.0 GF93	1.58×10^4

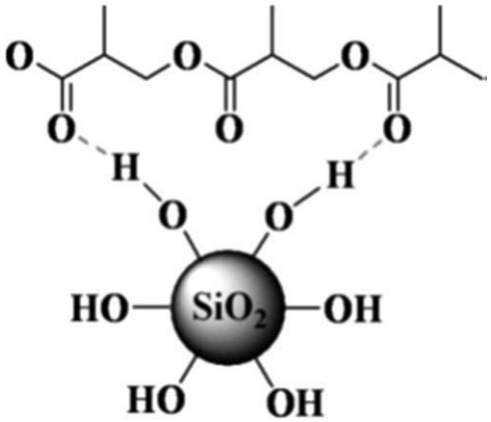

Figure 5. Hydrogen-bonding interactions between PLA and SiO_2.

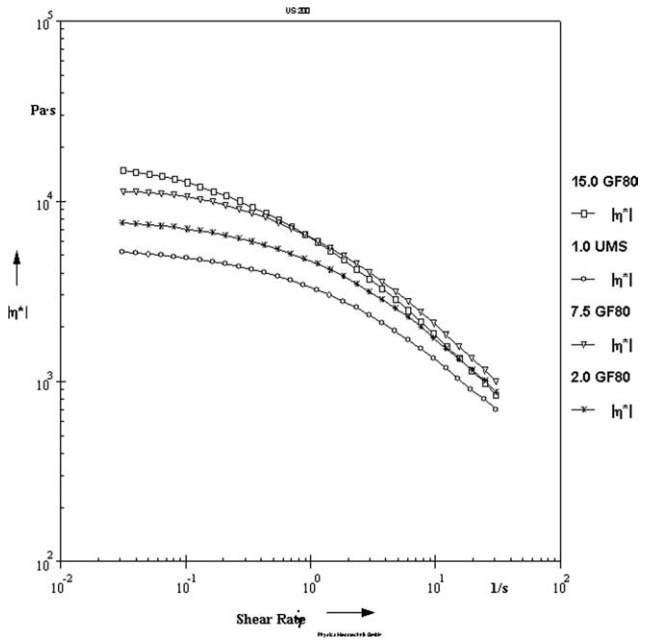

Figure 6. Rheology of GF80 samples compared to 1.0 UMS one.

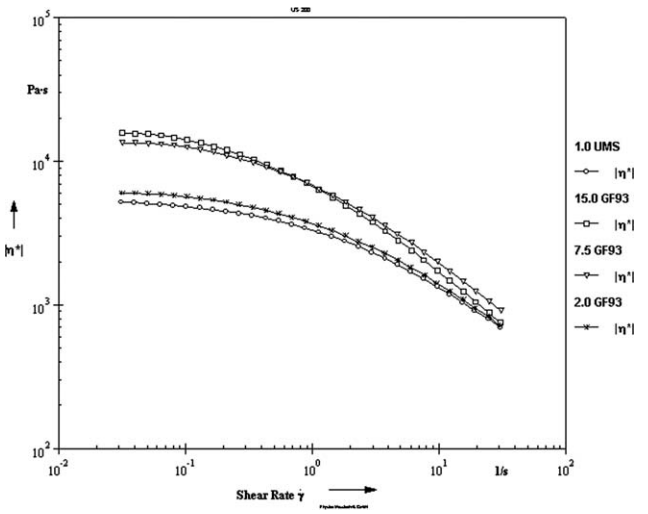

Figure 7. Rheology of GF93 samples compared to 1.0 UMS.

sample 2.0 UMS, with a low molecular weight has a comparable melt viscosity. The high values of η_0 of UMS samples can be due to the presence of hydrogen bonds between —Si—OH groups of silica and —C=O groups of PLA,[18] (Figure 5) thus altering the normal flow of PLA that flows with higher difficulty in the direction of flow, as reported by Zhu et al.[30]

It is important to underline that thanks to "in situ" synthesis the effects of silica on the viscosity are greatly enhanced. In previous articles dealing with melt compounding of PLA and nanosilica, higher quantities of nanosilica were required to reach viscosity values similar to the ones of neat PLA,[30] while with the "in situ" technique 0.5% only of nanosilica allows to obtain viscosity values far higher than those of neat PLA.

When silanes are present on the surface of silica (Figures 6 and 7), the effect on melt viscosity is magnified; both GF93 and GF80 increase melt viscosity at low shears. The different reactive

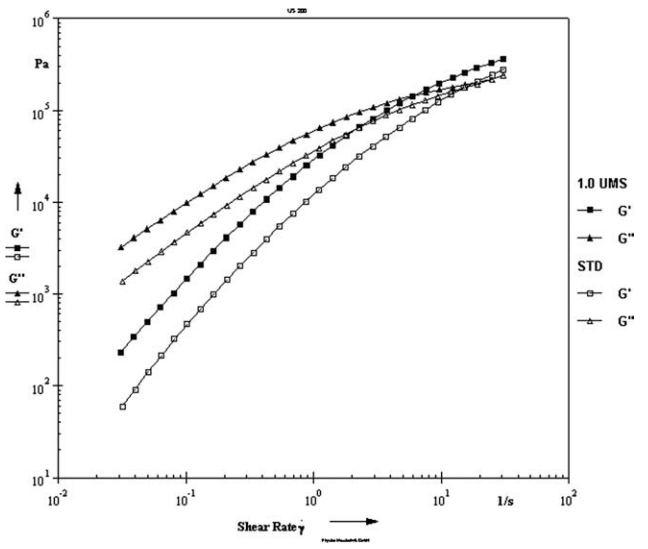

Figure 8. Storage (G′) and loss (G″) modulus of STD PLA and of 1.0 UMS.

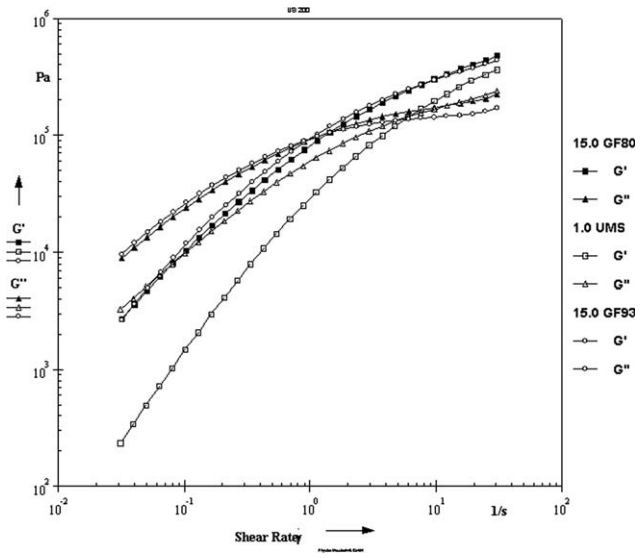

Figure 9. Storage (G′) and loss (G″) modulus of 1.0 UMS, 15.0 GF93 and 15.0 GF80.

groups on the surface of silica do not influence significantly melt viscosity; 15.0 GF93 and 15.0 GF80 have similar viscosities even if different reactive groups are available on the surface of nanosilica. Both these samples show a marked shear-thinning when increasing shear rates, and reach melt viscosities lower than the ones of other samples. The effect may be caused by the presence of stable covalent bonds between polymer macromolecules and the silanes that at low shears create a sort of network responsible for increasing viscosity. At higher shears the different surface energy of unmodified silica and PLA creates aggregation between mineral nanoparticles and generates small voids that slightly contribute in building up viscosity for UMS; when silane is present, bonds between polymer and silane act as compatibiliser and avoid the aggregation of silica and the formation of voids, lowering melt viscosity.

G′ and G″ data show that the presence of silica and of modified silica has a great effect on both modulus and on their relative values. When the mineral is present, the point of intersection between the two modulus shifts toward lower shear rate values (Figure 8). This result confirms the filler-network structure formed, as already stated in the cited article by Zhu et al.

This effect is further amplified when silane is present, as shown in Figure 9; moreover, modulus is independent on the kind of silane. This data seem to verify the hypothesis that when silane is present, a network is formed. To further confirm this assumption, at low shear rates the relative difference between the storage modulus of silane containing samples and UMS sample is much higher than the difference between the loss modulus.

CONCLUSION

PLA nanocomposites synthesized via "in situ" bulk ROP polymerization of L-lactide with nanosilica were obtained; to increase the compatibility between PLA and nanosilica, two different silanes (an amino and an epoxy derivative) were used to modify the surface of nanosilica.

Thanks to surface modification, 1% of nanosilica was enough to obtain improvements previously observed only with far higher quantities of mineral. When unmodified silica was added M_n of the polymers were observed drop quickly, while silanes allow to obtain good values of molecular weights of the polymers and greatly enhance dispersion of the mineral in the polymeric matrix.

Melt viscosity is greatly affected by silica and silanes; at low shears nanocomposites containing surface-modified silica have very high η_0 values, that are caused by the reactions between the silane present on the surface of nanosilica and polymeric chains, creating a sort of network that increases viscosity. On the contrary at higher shear rates, high quantities of silane contribute in lowering melt viscosity because silanes avoid the aggregation of silica and the formation of voids between the mineral and the polymer. The values of storage and loss modulus confirm this hypothesis.

ACKNOWLEDGMENTS

This work has been carried on thanks to the financial support of *Fondazione Cariplo*, for the project "Nanocomposite PLA with complex macromolecular architecture for high performances in packaging."

REFERENCES

1. Hartmann, M. H. Biopolymers from Renewable Resources, Kaplan, D. L. Springer: Berlin, **1998; pp 367–411.**
2. Martin, O.; Averous, L. *Polymer* **2001,** *42*, 6209.
3. Ray, S. S.; Bousmina, M. *Prog. Mater. Sci.* **2005,** *8*, 962.
4. Sinha Ray, S.; Yamada, K.; Okamoto, M.; Ogami, A.; Ueda, K. *Chem. Mater.* **2003,** *7*, 1456.
5. Lebaron, P. C.; Wang, Z.; Pinnavaia, T. *J. Appl. Clay Sci.* **1999,** *15*, 11.
6. Guo, H.; Sreekumar, T. V.; Liu, T.; Minus, M.; Kumar, S. *Polymer* **2005,** *46*, 3001.
7. Kim, I.; Jeong, Y. G. *J. Polym. Sci. Part B: Polym. Phys.* **2010,** *48*, 850.
8. Chow, W. S.; Lok, S. K. *J. Therm. Anal. Cal.* **2009,** *95*, 627.
9. Meneghetti, P.; Shaikh, S.; Qutubuddin, S.; Nazarenko, S. *Rubber Chem. Tech.* **2008,** *81*, 821.
10. Fukushima, K.; Abbate, C.; Tabuani, D.; Gennari, M.; Camino, G. *Polym. Deg. Stab.* **2009,** *94*, 1646.
11. Bronco, S.; Coltelli, B.; Castiello, S.; Ciardelli, F.; Taburoni, E.; Conzatti, L. *AIP Conf. Proc.* **2010,** *1255*, 67.
12. Chen, N.; Feng, H.; Luo, H.; Zhao, D.; Qiu, J. *Adv. Mat. Res. (Adv. Polym. Process.)* **2010,** *87–88*, 422.
13. Zhen, W.; Ma, X.; Yuan, L.; Pang, G.; Liu, Y. *Zhongguo Suliao* **2008,** *22*, 28.
14. Cohn, A.; Hotovely, S. *Biomaterials* **2005,** *26*, 2297.
15. Wu, T. M.; Wu, C. Y. *Polym. Degrad. Stab.* **2006,** *91*, 2198.
16. Pluta, M.; Jeszka, J. K.; Boiteux, G. *Eur. Polym. J.* **2007,** *43*, 2819.
17. Katiyar, V.; Navanati, H. *Polym. Comp.* **2011,** *32*, 497.

18. Wen, X.; Lin, Y.; Han, C.; Zhang, K.; Ran, X.; Li, Y.; Dong, L. *J. Appl. Polym. Sci.* **2009,** *114*, 3379.
19. Wen, X.; Lin, Y.; Han, C.; Li, Y.; Dong, L. *Macromol. Mater. Eng.* **2010,** *295*, 415.
20. Huang, J. W.; Yung, C. H.; Ya-Lan, W.; Chiun-Chia, K.; Mou-Yung, Y. *J. Appl. Polym. Sci.* **2009,** *112*, 1688.
21. Huang, J. W.; Yung, C. H.; Ya-Lan, W.; Chiun-Chia, K.; Mou-Yung, Y. *J. Appl. Polym. Sci.* **2009,** *112*, 3149.
22. Joubert, M.; Delaite, C.; Bourgeat-Lami, E.; Dumas, P. *J. Polym. Sci Part A: Polym. Chem.* **2004,** *42*, 1976.
23. Zhou, H. O.; Shi, T. *J. Polym. Mater. Sci. Eng.* **2006,** *22*, 220.
24. Liu, L. Z.; Ma, H. J.; Zhu, X. S. *Pigm. Res. Technol.* **2010,** *39/1*, 27.
25. Sun, Y.; Zhang, Z.; Wong, C. P. *J. Colloid Interface Sci.* **2005,** *292*, 436.
26. Jalabert, M.; Fraschini, C.; Prud'Homme, R. E. *J. Polym. Sci. (A)* **2007,** *45*, 1944.
27. Li, D.; Liu, G.; Wang, L.; Shen, Y. *Polym. Bull.* **2011,**
28. Ki, W. K.; Seong, I. W. *Macromol. Chem. Phys.* **2002,** *203*, 2245.
29. Munstedt, H.; Koppl, T.; Trieber, C. *Polymer* **2010,** *51*, 185.
30. Zhu, A.; Diao, H.; Rong, Q.; Cai, A. *J. App. Pol. Sci.* **2010,** *116*, 2866.